Feriel Aouatef Sahki, Mehdi Bouchouit, Sofiane Bouacida, Lyamine Messaadia, Elsa Caytan, Aissa Chibani, Thierry Roisnel and Abdelmalek Bouraiou*

Three metal(II) complexes constructed using the 2-(1*H*-benzo[*d*]imidazol-2-yl)quinoline ligand

https://doi.org/10.1515/znb-2021-0071
Received May 8, 2021; accepted July 10, 2021;
published online August 6, 2021

Abstract: 2-(1*H*-benzo[*d*]imidazol-2-yl)quinoline (BQ) as ligand and three coordination compounds of formula $\{Zn(BQ)Cl_2\}$ (**1**), $\{Pb(BQ)Cl_2\}_n$ (**2**) and $\{[Cu(BQ)_2(OC(O)CH_3)]OC(O)CH_3 \cdot CH_3COOH\}$ (**3**) have been synthesized and fully characterized. The complexes crystallize in triclinic space group $P\bar{1}$. In complexes **1** and **2**, the coordination geometry is a distorted tetrahedral environment around the zinc center and a distorted sixfold coordination geometry around the lead center, respectively. In complex **3** the central Cu(II) center is in a trigonal bipyramidal coordination geometry. The Cu(II) ion is surrounded by two bidentate 2-(2′-quinolyl) benzimidazole (BQ) ligands and one coordinated acetate molecule. One further acetate anion associated by a strong hydrogen bond with a molecule of acetic acid balances the charge of the compound.

Keywords: benzimidazole; copper(II); coordination compounds; lead(II); single-crystal X-ray diffraction; zinc(II).

1 Introduction

Rational design, synthesis, and structural characterization of new functional coordination compounds have received considerable attention in recent years [1, 2]. The design of new metal complexes was focused on designing the ligand structure and its functionality towards the metal center [3]. The current interest in coordination compounds is due to their intriguing variety of architectures and topologies and their versatile applications as functional materials.

For the creation of more coordination compounds, several ligands with multi-N-donor atoms were used [4, 5]. In this context, the use of nitrogen-rich heterocyclic compounds has attracted significant attention [6, 7]. Currently, several complexes containing heterocyclic nitrogen-donor ligands have been extensively investigated experimentally and theoretically [8–10]. The ligand 2-(2′-quinolyl)benzimidazole has been used to prepare several coordination compounds and detect metal ions [11–13]. Furthermore, several types of research have shown that their Ni, Cu, Ir, Re, Pd, Ti, Zn, and Ru complexes have good optoelectronic and catalytic properties [14, 15].

In our present work and as part of our recent research effort [16–18], quinoline, known as having desirable photophysical properties as a fluorophore group, and benzimidazole, were combined into one molecule 2-(1*H*-benzo[*d*]imidazol-2-yl)quinoline (BQ) (Scheme 1) which can be used for the construction of new zinc, lead and copper coordination complexes. X-ray crystallographic analysis, elemental analysis, UV and IR spectra have been used to characterize these new metal complexes. Recently, several crystal structures of metal complexes with the ligand **BQ** were reported [18, 19] (Scheme 1). Here, we describe the synthesis and structural determination of new zinc (**1**), lead (**2**), and copper (**3**) complexes obtained with the 2-(2′-quinolyl)benzimidazole ligand BQ.

2 Results and discussion

The BQ ligand was prepared following the established methods. The spectroscopic results and physical properties are in good agreement with literature reports [18, 20]. The ligand BQ was stirred in MeOH with 1 equivalent of MCl_2 (M = Zn and Pb) overnight at room temperature (Scheme 2). The metal(II) complexes **1** and **2** were filtered off and dried.

***Corresponding author: Abdelmalek Bouraiou,** Unité de Recherche de Chimie de l'Environnement et Moléculaire Structurale, Université des Frères Mentouri, Constantine 25000, Algeria,
E-mail: bouraiou.abdelmalek@umc.edu.dz
Feriel Aouatef Sahki, Mehdi Bouchouit and Aissa Chibani, Unité de Recherche de Chimie de l'Environnement et Moléculaire Structurale, Université des Frères Mentouri, Constantine 25000, Algeria
Sofiane Bouacida, Unité de Recherche de Chimie de l'Environnement et Moléculaire Structurale, Université des Frères Mentouri, Constantine 25000, Algeria; and Département Sciences de la Matière, Université Oum El Bouaghi, 04000 Oum El Bouaghi, Algeria
Lyamine Messaadia, Laboratoire Énergétique Appliquée et Matériaux, Université de Jijel, 18000 Jijel, Algerie
Elsa Caytan, CNRS, ISCR-UMR6226, Université de Rennes 1, Campus de Beaulieu, F-35000, Rennes, France
Thierry Roisnel, Institut des Sciences Chimiques de Rennes, UMR 6226, Université de Rennes 1, Campus de Beaulieu Bâtiment 10B, Bureau, 15335042 Rennes, France

The copper complex **3** was obtained by reacting BQ ligand and copper(II) acetate in MeOH. All complexes are stable in the air, soluble in DMF and DMSO, but insoluble in water and other organic solvents. The crystals of complexes **1** and **2** were obtained from the crystallization of the crude products in DMF. Complex **3** is crystallized in a mixture of acetic acid and isopropanol. The complexes **1**, **2**, and **3** were characterized by IR, UV/Vis spectroscopy, single-crystal X-ray diffraction, and elemental analysis.

To establish the structure of the coordination compounds, single-crystal X-ray diffraction analyses of complexes **1–3** were undertaken. The crystal structures with the atom numbering scheme are shown in Figures 1a, 2a and 3a. All complexes **1**, **2**, and **3** crystallize in the triclinic crystal system, space group $P\bar{1}$ (Table 1). In complexes **1** and **2**, the M(II) metal center is surrounded by two chlo rine atoms and one bidentate 2-(1*H*-benzo[*d*]imidazol-2-yl) quinoline ligand. The M–Cl, and M–N bond lengths for these complexes were found to be within their expected range (Table 2). The coordination of the BQ ligands at the metal(II) centers are very similar in complexes **1** and **2** and are comparable to previously reported structures [18]. The molecule of BQ consists of a benzimidazole ring with a quinoline ring in the two-position of the benzimidazole. In the benzimidazole ring, the N=C imine bond length {1.318(3) Å for 1, 1.330(3) Å for **2** and 1.331(5)–1.329(5) Å for **3**} is shorter than the amine N–C bond length {1.336(3) Å for **1**, 1.357(3) Å for **2** and 1.380(5)–1.384(5) Å for **3**}, as expected. Other bond lengths and angles of BQ exhibit no unusual features. The benzimidazole and quinoline rings of the BQ ligand almost share a common plane with a dihedral angle of 0.65(1)° for **1**, 10.14(2)° for **2**, and 2.836(1)° for **3** [18].

In complex **1**, the coordination geometry at the metal center is a distorted tetrahedral environment. The packing of the molecules in **1** can be described as alternating layers parallel to the crystallographic (001) plane along the *a* axis (Figure 1b). The molecules are linked via N–H···Cl intermolecular hydrogen bonds forming an infinite one-dimensional network in one line generating a $R_{FX}(1)$ motif ring (Figure 1b, Table 3). The crystal structure is also stabilized by intermolecular π–π stacking Cg–Cg (center of gravity) between aromatic rings. The shortest centroid-centroid distance is 3.6762(16) Å (Figure 1c).

The structural unit of complex **2** contains one {Pb(BQ)Cl_2} fragment and consists of a polymeric chain extending along the *a* axis, in which the Pb^{II} atoms are linked in first instance to two nitrogen atoms of BQ and two chlorine atoms (Table 2, Figure 2a). Both chlorine atoms act further as bridging ligands between Pb(II) centers with distances between Pb(1) and $Pb(1)^{i/ii}$ being 4.3786(1) and 4.6036(2) Å, respectively (for symmetry operations i and ii see Table 2). The bridging angles Pb(1)–Cl(1)–$Pb(1)^{ii}$ and Pb(1)–Cl(2)–$Pb(1)^{i}$ are 100.10(2)° and 98.84(2)°, respectively. Complex **2** exhibits a distorted six-fold coordination geometry around the metal center, as is seen in Figure 2b. The polymeric chains are connected via N–H···Cl and C–H···Cl hydrogen bond (Figure 2c, Table 3).

In addition, it can be observed that the Pb atoms take part in very weak intramolecular interactions with the aromatic H(2) atom of the quinoline ligand with the angle C(2)–H(2)···Pb(1) being 122.49(19)° and the

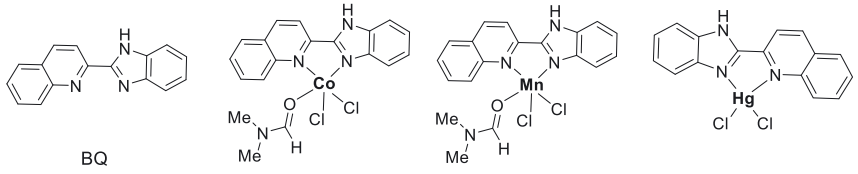

Scheme 1: Metal complexes with the BQ ligand reported in earlier studies [18].

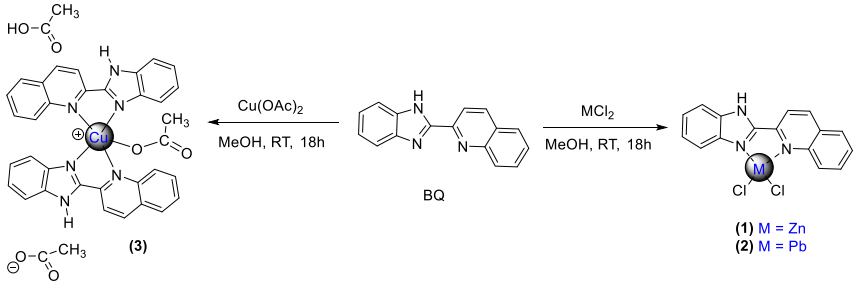

Scheme 2: Synthesis of **1**, **2** and **3**.

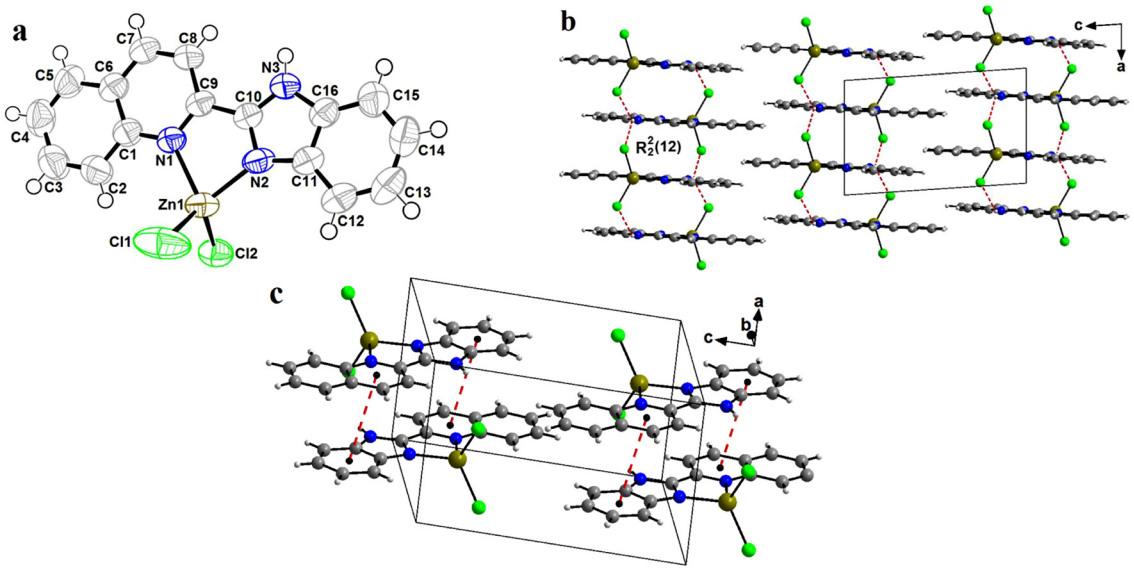

Figure 1: Plots of the molecular structure, hydrogen bonding interactions, π–π stacking interactions and packing of the molecules in **1**. (a) The molecular structure of **1** with the atom numbering scheme adopted. Displacement ellipsoids are drawn at the 50% probability level. (b) Projection along the *b* axis of the atomic arrangement of **1**. Dotted lines in red represent the N–H···Cl hydrogen bond. (c) Crystal structure highlighting the π–π stacking interactions between two quinolyl planes.

distance H(2)···Pb(1) being 3.163(1) Å (Table 4). In addition, there are C–H···π and π–π interactions, the lat ter with the shortest centroid-centroid distance of 3.5495(19) Å between the quinolyl rings. These interactions give rise to the formation of a polymeric two-dimensional network. The interactions are much weaker than the coordinative bonds but play an essential role in creating multidimensional networks in the solid state, as is shown in the present case.

X-ray data revealed that the asymmetric unit of complex **3** has a penta-coordinated copper center. The metal atom is surrounded by two bidentate 2-(2′-quinolyl)benzimidazole (**BQ**) ligands and one monodentate O-coordinated acetate molecule (Table 2). One further acetate anion balances the charge. An acetic acid molecule is also present in the crystals (Figure 3a). The ligand **BQ** acts as a bidentate ligand and coordinates the copper atom by the N(1A)/N(1B) and N(2A)/N(2B) atoms. The two coordinated **BQ** ligands are almost planar and form a dihedral angle of 69.27(1)°. The coordination sphere of the copper center can be described as a trigonal bipyramidal geometry: the atoms N(2A), N(2B), and O(21) form the equatorial plane, and N(1A), N(1B) are in the axial positions. The deviation of the copper atom from the equatorial plane is 0.0912 Å.

The packing in the crystal can be described as alternating layers along the crystallographic [110] direction parallel to the ($\bar{1}$10) planes. In these layers, the arrangement of the molecules is induced by strong intermolecular π–π stacking interactions. The shortest centroid–centroid distance is 3.520(3) Å (Figure 3b). Hydrogen bonding also plays a crucial role in consolidating the crystal structure of complex **3** (Table 3). Also, this complex presents N–H···O, O–H···O and weaker C–H···O hydrogen bonds forming chains and rings, respectively, with graph set motifs $D_{FX}(2)$, $D_{FX}(2)$ and $S_{FX}(8)$. These interactions allow the formation of layers of molecules and support the stacking of these layers (Figure 3a).

3 Conclusion

This paper describes the synthesis and the single-crystal X-ray diffraction analysis of complexes of the 2-(2′-quinolyl)benzimidazole ligand with Zn(II), Pb(II) and Cu(II) centers. The preparation is successful with simple, conventional methods. In {$Zn(BQ)Cl_2$} (**1**), the coordination geometry at the zinc center is a distorted tetrahedral environment. Complex **2** has a distorted sixfold coordination geometry around the lead center. Both molecular complex (**1**) and coordination polymer (**2**) show significant N–H···Cl interactions, while in crystals of complex (**2**) C–H···Cl interactions appear to support the aggregation. The third complex {$Cu(BQ)_2(OC(O)CH_3)OC(O)CH_3$, CH_3COOH} (3) shows trigonal bipyramidal coordination

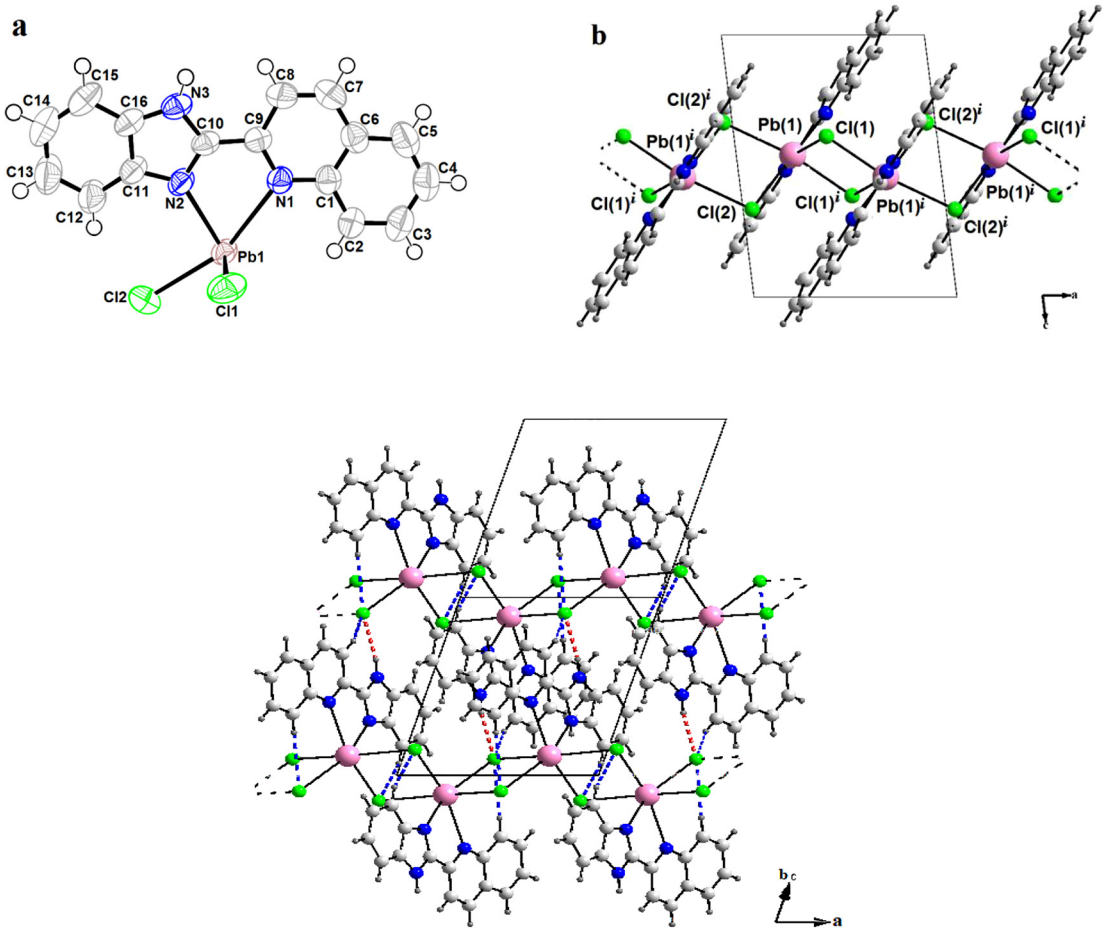

Figure 2: Plots of the asymmetric unit of compound **2**, the polymeric chains and the hydrogen bonding interactions in the packing of the molecules in the solid state. (a) The molecular structure of **2** with the atom numbering scheme adopted. Displacement ellipsoids are drawn at the 50% probability level. (b) Packing in the solid state viewed along the *b* axis (symmetry-equivalent atoms i are generated by centers of inversion with the symmetry operations $-x+2, -y+1, -z+1$ and $-x+1, -y+1, -z+1$). (c) View of the crystal structure showing the hydrogen bond interactions N–H···Cl and C–H···Cl as red and blue dashed lines, respectively.

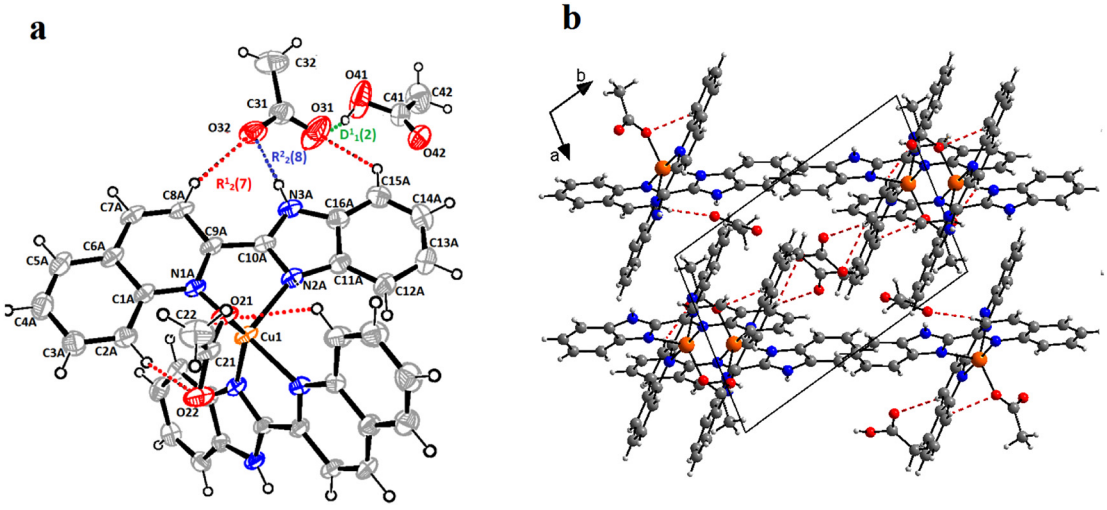

Figure 3: Plots of the molecular structure, packing of the molecules in the solid state and hydrogen bonding interactions of **3**. (a) The molecular structure of **3** with the atom numbering scheme adopted. Displacement ellipsoids are drawn at the 50% probability level. (b) The crystal structure viewed along the *c* axis, showing N–H···O, O–H···O and C–H···O interactions as dashed lines.

Table 1: Crystal structure data for complexes **1**, **2** and **3**.

	{Zn(BQ)Cl_2} (1)	{Pb(BQ)Cl_2}$_n$ (2)	{[Cu(BQ)$_2$(OC(O)CH_3)] OC(O)CH_3·CH_3COOH} (3)
Formula	$C_{16}H_{11}Cl_2N_3Zn$	$C_{16}H_{11}Cl_2N_3Pb$	C_{38} $H_{32}CuN_6O_6$
Formula weight	381.55	523.38	732.24
Crystal habit, color	Prism, yellow	Prism, colorless	Prism, green
Crystal system	tricLinic	Triclinic	Triclinic
Space group	$P\bar{1}$	$P\bar{1}$	$P\bar{1}$
a, Å	7.2372(2)	8.1709(1)	9.3887(8)
b, Å	9.3947(3)	10.1495(2)	13.2627(11)
c, Å	11.5114(3)	11.1759(2)	15.0857(12)
α, °	85.1100(10)	66.383(1)	100.280(5)
β, °	86.183(2)	77.533(2)	106.141(5)
γ, °	89.4560(10)	74.579(1)	100.278(5)
Volume, Å^3	778.09(4)	812.33(2)	1723.0(2)
Z, Z'	2, 2	2, 2	2, 2
D_{calcd}, g cm^{-3}	1.63	2.14	1.41
μ(Mo$K\alpha$), mm^{-1}	1.9	10.7	0.7
F(000), e	384	488	758
Crystal size, mm^3	0.16 × 0.08 × 0.05	0.12 × 0.12 × 0.11	0.08 × 0.11 × 0.19
θ range data collection, °	2.82–27.24	3.09–32.21	2.49–22.72
Reflections collected	9336	19,937	11,952
Independent reflections	3482	5611	5966
R_{int}	0.0242	0.0213	0.0716
Reflections with $I > 2\sigma(I)$	3334	5086	4130
Number of parameters	199	199	464
Goodness-of-fit on F^2	1.042	1.051	1.09
Final $R1$ [$I > 2\sigma(I)$]	0.0333	0.0212	0.0228
$R1$/$wR2$ (all data)	0.045/0.0902	0.0257/0.0462	0.1002/0.1681
Largest diff. peak/hole, Å^{-3}	0.34/−0.37	1.94/−0.63	1.36/−0.88
CCDC deposition no.	CCDC 1478614	CCDC 1478613	CCDC 1455170

Table 2: Selected bond lengths (Å) and angles (°) in complexes **1**, **2** and **3** in the solid state.

{Zn(BQ)Cl_2} (1)		{Pb(BQ)Cl_2}$_n$ (2)		{[Cu(BQ)$_2$(OC(O)CH_3)] OC(O)CH_3·CH_3COOH} (3)	
Bond lengths					
Zn(1)–N(1)	2.1066(18)	Pb(1)–N(1)	2.708(2)	Cu(1)–N(1A)	2.019(3)
Zn(1)–N(2)	2.034(2)	Pb(1)–N(2)	2.486(2)	Cu(1)–N(2B)	2.043(4)
Zn(1)–Cl(1)	2.2047(8)	Pb(1)–Cl(1)	2.7920(8)	Cu(1)–N(1B)	2.053(3)
Zn(1)–Cl(2)	2.2111(6)	Pb(1)–Cl(2)	2.7755(7)	Cu(1)–N(2A)	2.146(3)
C(10)–N(2)	1.318(3)	Pb(1)–Cl(1)^{ii}	3.2034(8)	Cu(1)–O(21)	1.974(3)
C(10)–N(3)	1.336(3)	Pb(1)–Cl(2)^{i}	2.9868(8)	O(21)–C(21)	1.274(5)
Bond angles					
N(2)–Zn(1)–N(1)	80.69(7)	N(2)–Pb(1)–N(1)	64.75(7)	N(2B)–Cu(1)–N(1B)	81.33(13)
N(2)–Zn(1)–Cl(1)	120.00(6)	N(2)–Pb(1)–Cl(2)	94.16(5)	N(1A)–Cu(1)–N(1B)	177.02(13)
Cl(1)–Zn(1)–Cl(2)	111.55(3)	Cl(1)–Pb(1)–Cl(2)	93.19(2)	N(1A)–Cu(1)–N(2B)	95.94(13)
		N(1)–Pb(1)–Cl(2)^{i}	95.38(4)	N(1A)–Cu(1)–N(2A)	80.17(13)
		Cl(2)–Pb(1)–Cl(2)^{i}	81.16(2)	O(21)–Cu(1)–N(2A)	108.49(13)
		Pb(1)–Cl(1)–Pb(1)^{ii}	100.10(2)	O(21)–Cu(1)–N(2B)	142.36(13)
		Pb(1)–Cl(2)–Pb(1)^{i}	98.84(2)	O(21)–C(21)–O(22)	123.5(4)
		Cl(1)–Pb(1)–Cl(2)^{i}	167.39(2)		

Symmetry code for **2**: (i) $-x + 2$, $-y + 1$, $-z + 1$; (ii) $-x + 1$, $-y + 1$, $-z + 1$.

Table 3: Distances (Å) and angles (°) for hydrogen bonds in crystals of **1**, **2** and **3**.

D···A	*d*(D–H)	*d*(H···A)	*d*(D–A)	D–H···A	Symmetry operation A
{Zn(BQ)Cl_2} (1)					
N(3)–H(3N)···Cl(1)	0.86	2.59	3.236(2)	132	$-x$, $1-y$, $2-z$
N(3)–H(3N)···Cl(2)	0.86	2.63	3.328(2)	139	$1-x$, $1-y$, $2-z$
{Pb(BQ)Cl_2}$_n$ (2)					
N(3)–H(3N)···Cl(1)	0.86	2.35	3.192(2)	165	$1-x$, $2-y$, $1-z$
C(2)–H(2)···Cl(1)	0.93	2.82	3.739(3)	169	$1-x$, $1-y$, $1-z$
C(4)–H(4)···Cl(2)	0.93	2.81	3.561(3)	138	$-1+x$, y, $1+z$
C(12)–H(12)···Cl(2)	0.93	2.77	3.613(8)	151	x, y, z
{[Cu(BQ)$_2$(OC(O)CH_3)]OC(O)CH_3·CH_3COOH} (3)					
N(3A)–H(3A)···O(32)	0.86	1.81	2.661(5)	172	x, y, z
N(3B)–H(3B)···O(22)	0.86	1.82	2.669(4)	167	$1-x$, $-y$, $1-z$
O(41)–H(41)···O(31)	0.82	1.80	2.480(8)	139	x, y, z
C(2A)–H(2A)···O(22)	0.93	2.58	3.368(6)	143	x, y, z
C(2B)–H(2B)···O(21)	0.93	2.40	3.013(6)	123	x, y, z
C(5A)–H(5A)···O(41)	0.93	2.54	3.224(8)	133	$2-x$, $-y$, $-z$
C(7A)–H(7A)···O(21)	0.93	2.49	3.209(5)	134	$1-x$, $-y$, $-z$
C(7B)–H(7B)···O(42)	0.93	2.52	3.304(6)	142	$2-x$, $1-y$, $1-z$
C(8A)–H(8A)···O(32)	0.93	2.38	3.258(7)	158	x, y, z
C(8B)–H(8B)···O(22)	0.93	2.37	3.225(6)	153	$1-x$, $-y$, $1-z$
C(15A)–H(15A)···O(31)	0.93	2.57	3.291(8)	135	x, y, z

of the metal(II) center. Crystals of this complex also feature N–H···O, O–H···O and C–H···O interactions.

4 Experimental section

4.1 General

All reagents, unless otherwise stated, were purchased as analysis grade and were used without further purification. The melting points were determined using an Electrothermal IA9100 digital melting point apparatus. UV spectra were recorded on a UV/VIS spectrophotometer Optizen 1220. Elemental analyses were performed on a Thermo Fisher FLASH 1112 (ISCR) elemental analyzer. Infrared (IR) samples were prepared as KBr pellets and their spectra were obtained in the range 400–4000 cm^{-1} on a Shimadzu FT/IR-8201 PC spectrophotometer.

4.2 X-ray crystallography

Crystallographic data for all the structures was collected on a Bruker APEX three-circle diffractometer equipped with an Apex II CCD detector using Mo*Kα* radiation (microfocus sealed tube with a graphite monochromator). The crystals were coated with Paratone oil and mounted on loops for data collection. The structures were solved by Direct Methods with SIR2004 [21] to locate all the non-H atoms which were subsequently refined anisotropically with SHELXL-97 [22] using full-matrix least-squares on F^2 from within the WINGX [23] suite of programs. Absorption corrections were performed with the program SADABS [24]. All non-hydrogen atoms were refined anisotropically. Hydrogen atoms were placed in idealized geometrical positions and refined with U_{iso} tied to the parent atom with the riding model.

CCDC 1478614, 1455170, and 1478613 contain the supplementary crystallographic data for complexes **1**, **2**, and **3**, respectively. These data can be obtained free of charge from The Cambridge Crystallographic Data Centre *via* www.ccdc.cam.ac.uk/data_request/cif.

Table 4: Distances (Å) and angles (°) for intramolecular interactions C–H···Pb in the crystal structure of {Pb(BQ)Cl_2}$_n$ (**2**).

C–H···Pb	*d* (C–H)	*d*(H···Pb)	*d* (C–Pb)	C–H···Pb	Symmetry operation Pb
C(2)–H(2)·Pb(1)	0.93	3.163(1)	3.74(2)	122.49(19)	x, y, z

4.3 Preparation of the ligand BQ and of the complexes 1, 2 and 3

4.3.1 Synthesis of 2-(1*H*-benzo[*d*]imidazol-2-yl)quinoline (BQ): 2-(1*H*-benzo[*d*]imidazol-2-yl)quinoline (BQ) has been synthesized in accordance with established methods [18]. Spectroscopic results and physical properties are in agreement with literature reports [18, 20].

4.3.2 Synthesis of {Zn(BQ)Cl_2} (1): Complex **1** was synthesized starting from a mixture of 2-(1*H*-benzo[*d*]imidazol-2-yl)quinoline (BQ) (1.0 mmol), $ZnCl_2$ (1.0 mmol) in 10 mL of MeOH at room temperature. Yield 83%; colorless powder, m.p. 210–217 °C. – Analysis for $C_{16}H_{11}N_3Cl_2Zn$: calcd. C 50.36, H 2.91, N 11.01; found C 49.76, H 2.86, N 10.68%. – UV/Vis (DMF): λ_{max} = 288, 310, 338, 352 nm – IR: 3444, 3228, 2349, 1596, 1500, 1446, 1326, 1145, 1014, 833, 752, 594 cm^{-1}.

Colorless crystals of **1** suitable for X-ray diffraction were obtained from dimethylformamide solution.

4.3.3 Synthesis of $\{Pb(BQ)Cl_2\}_n$ (2): Complex **2** was obtained in moderate yield (48% based on BQ) by a similar method as described for **1** except that $PbCl_2$ were used instead of $ZnCl_2$. Colorless powder, m.p. 208–215 °C. – UV/Vis (DMF): λ_{max} = 245, 287, 337, 351 nm – IR: 3390, 3055, 1596, 1500, 1411, 1315, 1269, 1145, 1103, 833, 752, 609 cm^{-1}. Colorless crystals of **3** suitable for X-ray diffraction were obtained from dimethylformamide solution.

4.3.4 Synthesis of $\{[Cu(BQ)_2(OC(O)CH_3)]OC(O)CH_3{\cdot}CH_3COOH\}$ (3): A mixture of $Cu(OAc)_2$ (1 mmol) and 2-(2′-quinolyl)benzimidazole (**BQ**) (2 mmol) was dissolved in 10 mL of MeOH. The mixture was stirred for 18 h. The precipitate was collected by filtration and dried *in vacuo*. Yield 67%; green powder, m.p. 310–315 °C. – UV/Vis (DMF): λ_{max} = 300, 368, 396 nm – IR: 2364, 1540, 1428, 1387, 1332, 995, 852, 751, 675 cm^{-1}. The crude product was recrystallized in isopropanol and a few drops of acetic acid to obtain single crystals suitable for X-ray diffraction.

Author contributions: All the authors have accepted responsibility for the entire content of this submitted manuscript and approved submission.

Research funding: This research received no specific grant from any funding agency in the public, commercial, or not-for-profit sectors.

Conflict of interest statement: The authors declare no conflicts of interest regarding this article.

References

1. Zhang X.-L., Guo C.-P., Yang Q.-Y., Wang W., Liu W.-S., Kang B.-S., Su C.-Y. *Chem. Commun.* 2007, *41*, 4242–4244.
2. Bodman S. E., Crowther A. C., Geraghty P. B., Fitchett C. M. *Cryst.Eng.Comm*. 2015, *17*, 81–89.
3. Lalegani A., Sardashti M. K., Khalaj M., Gajda R., Woźniak K. *Inorg. Chim. Acta* 2017, *457*, 136–144.
4. Maekawa M., Minamino A., Sugimoto K., Okubo T., Kuroda-Sowa T., Munakata M. *Inorg. Chim. Acta* 2014, *413*, 257–263.
5. Nasani R., Saha M., Mobin S. M. *Dalton Trans.* 2014, *43*, 9944–9954.
6. Crowley J. D., McMorran D. A. "Click-triazole" coordination chemistry: exploiting 1,4-disubstituted-1,2,3-triazoles as ligands. In *Topics in Heterocyclic Chemistry*; Košmrlj J., Ed.; Springer: Berlin, Heidelberg, Vol. 28, 2012; pp. 31–38.
7. Bernabé-Pablo E., Campirán-Martínez A., Jancik V., Martínez-Otero D., Moya-cabrera M. *Polyhedron* 2016, *110*, 305–313.
8. Cary D. R., Zaitseva M. P., Gray K., O'Day K. E., Darrow C. B., Lane S. M., Peyser T. A., Satcher J. H., Van Antwerp W. P., Nelson A. J., Reynolds J. G. *Inorg. Chem.* 2002, *41*, 1662–1669.
9. Tyson D. S., Henbest K. B., Bialecki J., Castellano F. N. *J. Phys. Chem. A* 2001, *105*, 8154–8161.
10. Sangilipandi S., Nagarajaprakash R., Sutradhar D., Kaminsky W., Chandra A. K., Rao K. M. *Inorg. Chim. Acta* 2015, *437*, 177–187.
11. Li G., Zhang D., Liu G., Pu S. *Tetrahedron Lett.* 2016, *57*, 5205–5210.
12. Zhao Y., Chai W. X., Song L., Zhang Y. C., Shi H. S., Tao X. D., Shu K. Y. *Phosphorus Sulfur Relat. Elem.* 2016, *191*, 1123–1128.
13. Zhang W. J., Huang W., Liang T. L., Sun W. H. *Chin. J. Polym. Sci.* 2013, *31*, 601–609.
14. Dayan O., Tercan M., Özdemir N. *J. Mol. Struct.* 2016, *1123*, 35–43 and references cited therein.
15. Gong D. P., Gao T. B., Cao D. K., Ward M. D. *Dalton Trans.* 2017, *46*, 275–286.
16. Bouchouit M., Bouraiou A., Bouacida S., Belfaitah A., Merazig H. *J. Struct. Chem.* 2016, *57*, 835–839.
17. Bouchouit M., Said M. E., Kara Ali M., Bouacida S., Merazig H., Kacem Chaouche N., Chibani A., Zouchoune B., Belfaitah A., Bouraiou A. *Polyhedron* 2016, *119*, 248–259.
18. Sahki F. A., Messaadia L., Merazig H., Chibani A., Bouraiou A., Bouacida S. *J. Chem. Sci.* 2017, *129*, 21–29.
19. Wang X., Fan R., Dong Y., Su T., Huang J., Du X., Wang P., Yang Y. *Cryst. Growth Des.* 2017, *17*, 5406–5421.
20. Mamedov V. A., Saifina D. F., Gubaidullin A. T., Ganieva V. R., Kadyrova S. F., Rakov D. V., Rizvanov I. K., Sinyashin O. G. *Tetrahedron Lett.* 2010, *51*, 6503–6506.
21. Burla M. C., Caliandro R., Camalli M., Carrozzini B., Cascarano G. L., De Caro L., Giacovazzo C., Polidori G., Spagna R. *J. Appl. Crystallogr.* 2005, *38*, 381–388.
22. Sheldrick G. M. *Acta Crystallogr* 2008, *A64*, 112–122.
23. Farrugia L. J. J. *Appl. Crystallogr.* 2012, *45*, 849–854.
24. Sheldrick G. M. SADABS; Bruker AXS Inc.: Madison, Wisconsin (USA), 2002.